Short Papers

Improved X-Band FM Discriminator

T. P. CHATTOPADHYAY AND B. N. BISWAS

Abstract—**The technique of coherent carrier-addition, using injection synchronization of a narrow-band Gunn oscillator, for improving the performance of an X-band frequency discriminator has been examined in detail. The discriminator is implemented from a single magic tee, two adjustable AM detectors, two sliding shorts, a circulator, an isolator, and a difference amplifier of gain unity. Experimental results are presented in partial support of the conclusions of the analysis. Normal operation of the discriminator in absence of the coherent carrier is also described as a special case of the above analysis.**

I. Introduction

The literature indicates a growing activity of scientists and engineers in designing discriminators at microwave frequencies since the early 1960's. Pound's discriminator [1], [2], incorporating a resonant cavity, had been used over a long period in the early days of microwave frequency discriminators. The wide-band transmission-line discriminators [3], [4] designed by Lee and Seo have been used up to 1 GHz. A flexible microwave phase discriminator has been implemented by Mohr [5] and discussed by Robinson [6]. Its analysis has been carried out later by assuming square law [7] and linear [8] operations of the component AM detectors. Developments of a stripline frequency discriminator [9] at L- and S-bands, and a waveguide discriminator [10] at X-band are seen as the next phase. A discriminator based on the principle of electrical phase control [11], [12] and a much simpler implementation [13] using a single magic tee have also been described. The latest implementation of a single hybrid tee microwave frequency discriminator is due to Peebles and Green [14], [15]. It uses a transmission line in order to achieve phase splitting between the two component waves. The present implementation which is identical with [14], [15] uses two sliding shorts and a waveguide line for the same. The bandwidth and the frequency sensitivity of the discriminator can be adjusted easily by varying the length of the waveguide line. The discriminator is analyzed by assuming both square law and linear operation of the AM detectors.

This paper describes an important technique for increasing the strength of the signal appearing at the discriminator output simply by adding a coherent carrier with the FM signal at the discriminator input. It is difficult to design a broad-band injection-locked amplifier for the power amplification of a wide-band FM signal. The technique is suitable and important for the demodulation of a wide-band, weak FM signal in a receiving system. The implementation may also be recommended at higher frequencies.

Manuscript received April 27, 1984; revised November 12, 1985 This paper was supported by the Ministry of Defence, Government of India

The authors are with Radionics Laboratory, Physics Department, Burdwan University, Burdwan 713 104, India.

IEEE Log Number 8407182.

II. Mechanism of System Operation

The discriminator along with the source of coherent carrier is shown in Fig. 1. The input signal which may be a pure FM wave or an FM wave accompanied by the coherent carrier is directed by a circulator into port 1 (i.e., H-arm) of the second magic tee. The FM signal and the coherent carrier each is now split into two identical components having equal amplitude and equal phase. These components, in turn, emerge from the ports 2 and 3 (also known as colinear arms) of the magic tee and are reflected back by the sliding shorts. No wave emerges from port 4 (i.e., E-arm). Each of the reflected waves is again split by the hybrid tee into two components of equal amplitude which emerge from ports 1 and 4. These components are in phase for the wave reflected from port 2 while they differ in phase by π radian for that reflected from port 3. Thus each of the FM signal and the coherent carrier generates a pair of waves at each of the ports 1 and 4 of the magic tee. The pair resulting from a particular wave may be termed as the corresponding pair. Now, apart from the phase difference introduced by the magic tee, a phase difference proportional to the difference in lengths of the shorted waveguides is introduced between a corresponding pair of waves. Thus in presence of the coherent carrier, four waves appear at each of the ports 1 and 4 of the hybrid tee which form the input signal for the AM detectors connected with the respective ports. The detector outputs are proportional to the magnitudes or to the squares of the magnitudes of their respective inputs. The difference amplifier of gain unity performs the subtraction of the detector outputs.

In order to generate the coherent carrier, a small fraction of the input FM signal is directed into a Gunn oscillator tuned at the FM carrier frequency through a magic tee and a variable attenuator. The effective Q-value of the oscillator is high so that the sidebands of the injected FM signal lie outside the lockband of the oscillator and it is injection locked to the carrier of the FM signal. The injection-locked Gunn oscillator acts as a narrow-band, tunable, active filter for the synchronizing FM carrier and generates the carrier only at its output, suppressing the sidebands [16] of the FM signal. Half of the input FM signal power incident at port 2 of the first magic tee emerges from the H-arm of the magic tee and is reflected back by the sliding short connected with the H-arm. The FM signal power appearing at the discriminator input is half of this reflected power. The phase difference between the coherent carrier and the FM carrier emerging from port 3 of the first magic tee is made zero by adjusting the sliding shorts S_1 and S_2.

III. Analysis

Using complex representation, the input FM signal and the coherent carrier can be written as

$$v_s(t) = R_e V_0 e^{j(w_0 t + m_f \sin w_m t)} \tag{1}$$

and

$$v_c(t) = R_e x V_0 e^{j(w_0 t + \varphi_c)} \tag{2}$$

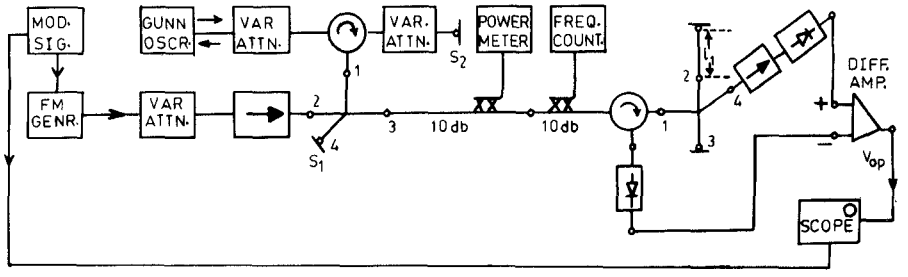

Fig. 1. Experimental arrangement for the X-band frequency discriminator.

respectively, where

- V_0 voltage amplitude,
- x ratio of voltage amplitudes of the coherent carrier and the FM signal,
- m_f index of frequency modulation,
- φ_c phase difference between the coherent carrier and the FM carrier,
- R_e real part.

w_0 and w_m are the angular frequencies of the carrier wave and the modulating signal, respectively. The phase velocity of the wave of angular frequency w inside the air-filled waveguide is given by

$$v_p(w) = c \Big/ \left(1 - \frac{w_{c0}^2}{w^2}\right)^{1/2}$$

where c is the velocity of light in air and w_{c0} is the cutoff frequency of the waveguide. If l_1 and l_2 are the lengths of the shorted waveguides in the two colinear arms of the magic tee, then the phase shifts of the FM signal and the coherent carrier in the waveguides are, respectively, given by

$$\varphi_k^s = \pi + \frac{2l_k w}{v_p(w)}$$

and

$$\varphi_k^c = \pi + \frac{2l_k w_0}{v_p(w_0)}$$

for $k = 1,2 \cdot \pi$ accounts for the phase change resulting from a reflection at the sliding short. Superscripts "s" and "c" stand for the FM signal and the coherent carrier, respectively. $w = w_0 + \Delta w$ where $\Delta w = m_f w_m \cos w_m t$ is the instantaneous frequency deviation of the FM signal.

In presence of the coherent carrier, the composite signal appearing at the inputs of the detectors connected with the H- and E-arms of the hybrid tee are, respectively, given by

$$v_1(t) = \frac{v_s(t)}{2} e^{-j\varphi_1^s}\left[1 + e^{j\alpha} + xe^{j\gamma}(1 + e^{j\beta})\right] \tag{3}$$

$$v_4(t) = \frac{v_s(t)}{2} e^{-j\varphi_1^s}\left[1 - e^{j\alpha} + xe^{j\gamma}(1 - e^{j\beta})\right] \tag{4}$$

where

$$\alpha = \frac{2w}{v_p(w)}(l_1 - l_2)$$

$$\beta = \frac{2w_0}{v_p(w_0)}(l_1 - l_2)$$

$$\gamma = \varphi_c - m_f \sin w_m t + \frac{2l_1 w}{v_p(w)} - \frac{2l_1 w_0}{v_p(w_0)}.$$

Now let $l_1 - l_2 = [v_p(w_0)/w_0](2n+1)(\pi/4)$ where $n = 0,1,2,\cdots$ etc. Then

$$\alpha = \sqrt{(w^2 - w_0^2)/g_1}\,(2n+1)\frac{\pi}{2w_0} \quad \text{and} \quad \beta = (2n+1)\frac{\pi}{2}$$

where $g_1 = 1 - (w_{c0}/w_0)^2$. Assuming, $\Delta w \ll w_0$ and using the binomial theorem we can write

$$\alpha = (2n+1)\frac{\pi}{2}\left[1 - \frac{\Delta w}{w_0 g_1}\right]$$

neglecting the squares and higher powers of $(\Delta w/w_0)$.

For simplicity, we consider the sliding short to be placed just at the end of port 3 of the discriminator magic tee. Then $l_2 = 0$. We also assume $\varphi_c = 0$.

A. Square Law Operation

Assuming square law operation of the detectors, the discriminator output is

$$V_{op} = \eta_1\left(|v_4|^2 - |v_1|^2\right) \tag{5}$$

where η_1 is the detector efficiency which is assumed to be the same for both the detectors.

Carrying out some mathematical manipulations and neglecting harmonics of an order higher than three, it is not difficult to show that

$$V_{op} = (-1)^n \cdot 2\eta_1 V_0^2\left[\{J_1(x_1) + xA_1\}\cos w_m t + xB_1 \sin w_m t + \{xD_1 - J_3(x_1)\}\cos 3w_m t + xE_1 \sin 3w_m t\right] \tag{6}$$

where

$$x_1 = (2n+1)\frac{\pi}{2}\frac{m_f w_m}{\omega_0 g_1}$$

$$A_1 = J_0(m_f)J_1(x_1) - \sum_{k=2}^{\infty}(-1)^k J_{2k-1}(x_1)J_{2k-2}(m_f) - \sum_{k=1}^{\infty}(-1)^k J_{2k-1}(x_1)J_{2k}(m_f)$$

$$B_1 = J_1(m_f) - J_0(x_1)J_1(m_f) - \sum_{k=1}^{\infty}(-1)^k J_{2k}(x_1)J_{2k+1}(m_f) + \sum_{k=1}^{\infty}(-1)^k J_{2k}(x_1)J_{2k-1}(m_f)$$

$$D_1 = J_1(x_1)J_2(m_f) - J_0(m_f)J_3(x_1) - \sum_{k=2}^{\infty}(-1)^k J_{2k-1}(x_1)J_{2k-2}(m_f) - \sum_{k=1}^{\infty}(-1)^k J_{2k-1}(x_1)J_{2k+2}(m_f)$$

$$E_1 = J_3(m_f) - J_0(x_1)J_3(m_f) + J_2(x_1)J_1(m_f) - \sum_{k=1}^{\infty}(-1)^k J_{2k}(x_1)J_{2k+3}(m_f) + \sum_{k=2}^{\infty}(-1)^k J_{2k}(x_1)J_{2k-3}(m_f). \tag{7}$$

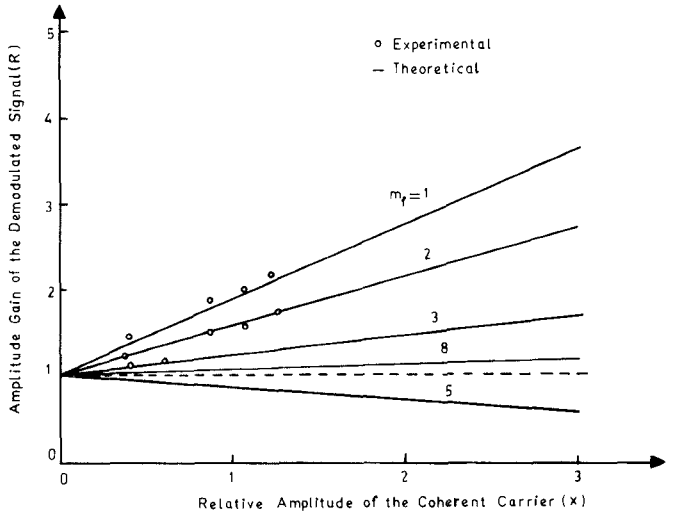

Fig. 2. Variation of the amplitude gain of the demodulated signal with relative amplitude of the coherent carrier under square law operation of the diode detectors. $n=18$, $f_0=9.356$ GHz, $f_m=0.1$ MHz Input FM signal power = 3 mW.

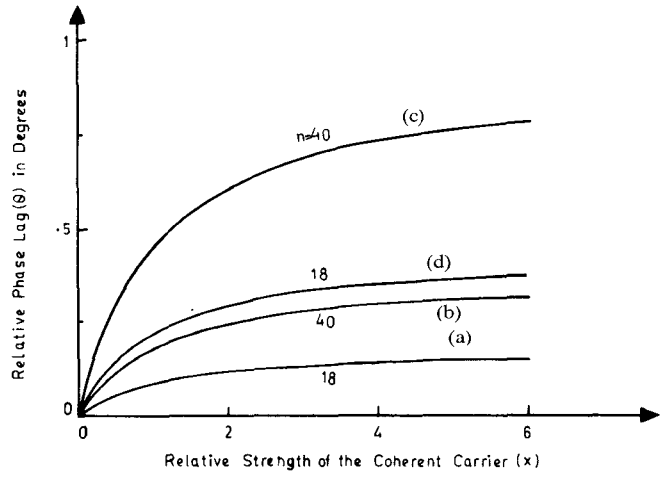

Fig. 3. Theoretical variation of the phase lag (θ) of the demodulated signal relative to the modulating signal with the relative amplitude of the coherent carrier assuming square law operation of the diode detectors. Curves (a) and (b). $m_f=1$, $f_m=1$ MHz. Curves (c) and (d): $m_f=0.5$, $f_m=10$ MHz.

$J_m(z)$ is the Bessel's function of order "m" and argument z. If R denotes the ratio of the demodulated signal amplitudes in presence and in absence of the coherent carrier, then

$$R=\frac{(V_{op})_{x\neq 0}}{(V_{op})_{x=0}}=\frac{\left[\{J_1(x_1)+xA_1\}^2+x^2B_1^2\right]^{1/2}}{J_1(x_1)} \tag{8}$$

while the phase lag θ of the demodulated signal relative to the modulating signal is given by

$$\tan\theta=\frac{xB_1}{J_1(x_1)+xA_1}. \tag{9}$$

Equation (8) shows that $R>1$ when $A_1>0$. Now, so far as the practical realization of the discriminator is concerned, $x_1\ll 1$ since increase of x_1 implies a proportional increase in the length of the waveguide line. So it is legitimate to assume that $J_1(x_1)\gg J_3(x_1)$ in practice. Considering low index modulation we get $A_1>0$ when $J_1(m_f)>0$. Thus the addition of the coherent carrier causes an enhancement of the demodulated signal amplitude provided $J_1(m_f)>0$. On the other hand, if $J_1(m_f)<0$, the coherent carrier produces an adverse effect and causes the demodulated signal amplitude to diminish. Again, since $J_1(m_f)$ is oscillatory in nature with gradually diminishing amplitudes, A_1 will have smaller positive values again at higher values of m_f. The numerical solution of (8), along with the experimental results are shown in Fig. 2, which shows that for a given index of modulation the change of the detected signal amplitude is directly proportional to the strength of the coherent carrier and that the amplitude enhancement favors low index of modulation. Phase lag θ is very small, but increases slowly with the increase of strength of the coherent carrier as shown in Fig. 3.

B. Distortion

Equation (6) indicates that in the presence of the coherent carrier the discriminator output contains odd harmonic distortions only. The third harmonic distortion is given by

$$D_c=\left[\frac{\{xD_1-J_3(x_1)\}^2+x^2E_1^2}{\{xA_1+J_1(x_1)\}^2+x^2B_1^2}\right]^{1/2}\times 100 \text{ percent} \tag{10}$$

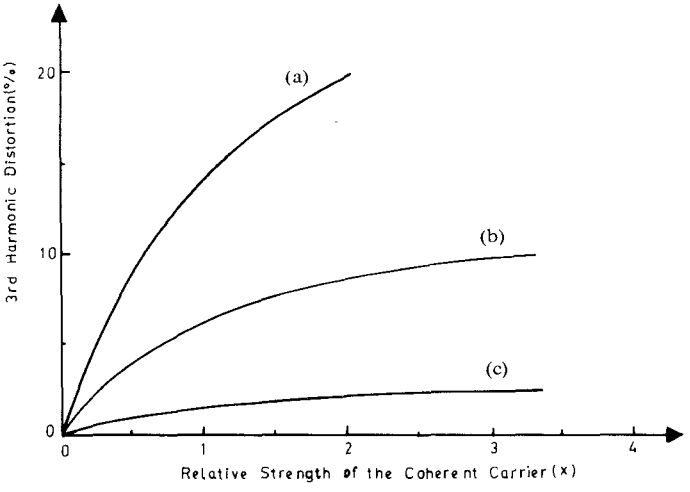

Fig. 4. Theoretical variation of third harmonic distortion with the relative amplitude (x) of the coherent carrier under square law operation of the AM detectors. $n=18$, $f_0=9356$ GHz. (a) $m_f=1.5$, (b) $m_f=1$, (c) $m_f=0.5$

where A_1, B_1, D_1, E_1 are functions of n, m_f, w_m, and w_0 as given in (7). Fig. 4 shows that for a given "m_f" and "n" third harmonic distortion increases with the increase of the coherent carrier strength and also that retaining the value of "n" unaltered if the modulation index is increased, the distortion increases rapidly. From the numerical solution of (10) it is seen that the third harmonic distortion does not vary appreciably with the value of "n" but it decreases slowly with increasing modulation frequency. Hence the distortion at the discriminator output can be minimized primarily by using a small index of modulation.

C. Linear Operation

Assuming linear operation of the AM detectors the discriminator output is given by

$$V_{op}=\eta_2(|v_4|-|v_1|) \tag{11}$$

where η_2 is the assumed same efficiency of the linear detectors.

Here

$$|v_1| = \frac{V_0}{\sqrt{2}}\left[1+\cos\alpha + x^2(1+\cos\beta) + x\{\cos\gamma + \cos(\beta-\gamma) + \cos(\alpha+\gamma) + \cos(\alpha-\beta+\gamma)\}\right]^{1/2} \quad (12)$$

$$|v_4| = \frac{V_0}{\sqrt{2}}\left[1-\cos\alpha + x^2(1-\cos\beta) + x\{\cos\gamma - \cos(\beta-\gamma) - \cos(\alpha+\gamma) + \cos(\alpha-\beta+\gamma)\}\right]^{1/2} \quad (12a)$$

It seems now difficult to derive an expression for V_{op} in a compact form. Neglecting the harmonic terms we can write

$$|v_1| = \frac{V_0}{\sqrt{2}}\left[A_0 - (-1)^n \cdot 2R_1 \cos(w_m t - \theta)\right]^{1/2} \quad (13)$$

and

$$|v_4| = \frac{V_0}{\sqrt{2}}\left[A_0 + (-1)^n \cdot 2R_1 \cos(w_m t - \theta)\right]^{1/2} \quad (14)$$

where

$$A_0 = 1 + x^2 + xJ_0(m_f)\{1 + J_0(x_1)\} + 2x\sum_{k=1}^{\infty}(-1)^k J_{2k}(x_1)J_{2k}(m_f)$$

$$R_1 = \sqrt{C_1^2 + C_2^2}$$

$$C_1 = J_1(x_1)\left[1 + xJ_0(m_f)\right] - x\sum_{k=2}^{\infty}(-1)^k J_{2k-1}(x_1)J_{2k-2}(m_f) - x\sum_{k=1}^{\infty}(-1)^k J_{2k-1}(x_1)J_{2k}(m_f)$$

$$C_2 = xJ_1(m_f)[1 - J_0(x_1)] + x\sum_{k=1}^{\infty}(-1)^k J_{2k}(x_1)J_{2k-1}(m_f)$$

and

$$\tan\theta = \frac{C_2}{C_1}. \quad (16)$$

Assuming $2R_1 \ll A_0$ and applying the binomial theorem, one can arrive at the following approximate expression:

$$V_{op} \simeq (-1)^n \eta_2 \sqrt{2}\, V_0 R_1 \cos(w_m t - \theta). \quad (17)$$

When $x = 0$, $R_1 = J_1(x_1)$ and $\theta = 0$.

Again, assuming $x_1 \ll 1$, (15) shows that $R_1/J_1(x_1) > 1$ when $J_0(m_f) > 0$. This, in turn, implies that the detected signal strength is increased in presence of the coherent carrier provided the modulation index of the input FM signal satisfies the condition $J_0(m_f) > 0$. All sorts of harmonic distortions are present in this case.

D. Discriminator Performance in Absence of the Coherent Carrier

Results in this section follow directly by putting $x = 0$ in the previous equations.

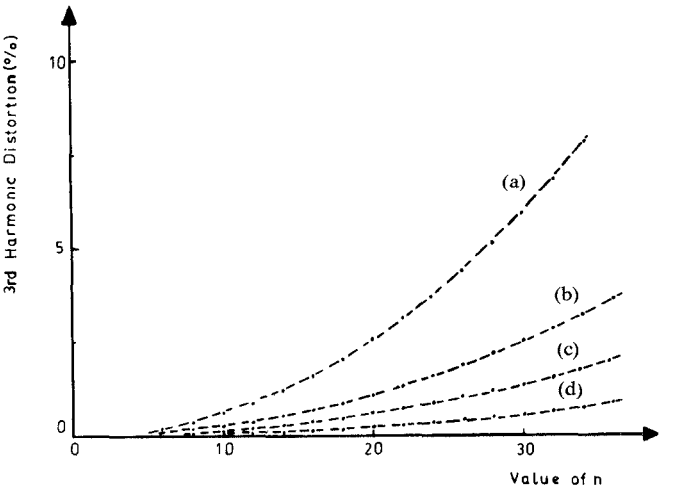

Fig. 5. Theoretical variation of third harmonic distortion with the value of "n" using frequency deviation (Δ) as the parameter in absence of the coherent carrier. Curves (a) and (c): $\Delta = 30$ MHz; Curves (b) and (d): $\Delta = 20$ MHz. Curves (a) and (b) assume square law operation while curves (c) and (d) assume linear operation of the diode detectors.

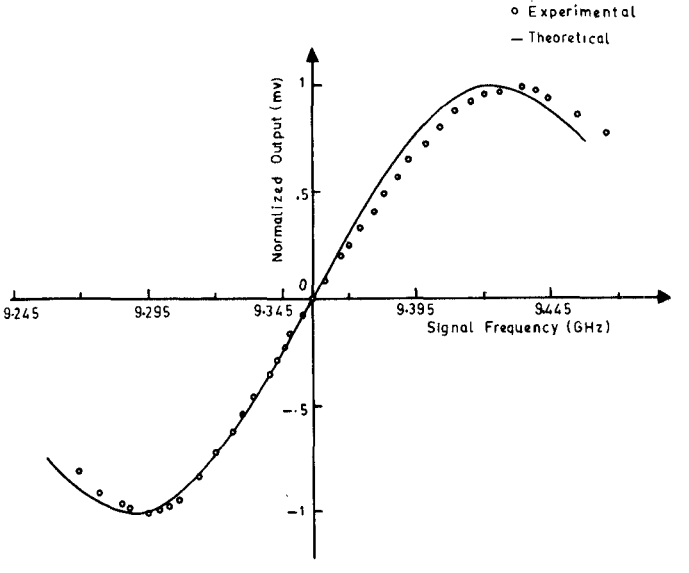

Fig. 6. Theoretical and experimental frequency response characteristics of the discriminator. Peak voltage output = 250 mV. Center frequency = 9.356 GHz, $n = 18$.

Under square law operation of the diode detectors, the discriminator output contains only the odd harmonic distortions. For a given frequency deviation, the variation of third harmonic distortion with "n" is shown in Fig. 5 which indicates that for small values of "n" the output is practically distortionless. The distortion, however, increases slightly with increasing "n."

Peaks in the frequency response of the FM discriminator occur at frequency deviations Δw given by

$$\frac{\Delta w}{w_0} = \pm g_1/(2n+1)$$

where $n = 0, 1, 2, \ldots$ etc.

The frequency band of the discriminator can be increased by using shorter waveguide lines and selecting the center frequency of the discriminator well above the cutoff frequency of the waveguide line used. The usable frequency band is a part of this band between peaks over which a fair linearity in exhibited. The

frequency sensitivity can be expressed as

$$S_{\text{sq law}} = \left.\frac{dV_{op}}{dw}\right|_{w=w_0} = (-1)^n \eta_1 V_0^2 (2n+1)\pi/(2w_0 g_1).$$

The frequency response characteristics of the discriminator under square law operation of the AM detectors is shown in Fig. 6. The length of the waveguide line used in the experiment is measured to be 28.6 cm·s. The corresponding value of "n" when calculated is 18. The sensitivity of this discriminator is found to be 5.7 mV/MHz for an input power level of 8 mW. The center frequency of this discriminator is 9.356 GHz and the peaks in the frequency response appear for frequency deviations of ± 68 MHz theoretically. Discriminator output as measured from a dual-trace oscilloscope is 250 mV at the response peaks. The measured output voltages are divided by a factor of 250 in order to normalize the response to a maximum value of unity.

Assuming linear operation of the envelope detectors, it is seen that the discriminator cannot be implemented with the difference in lengths of the shorted waveguides corresponding to the odd integral values of "n." The discriminator implemented with an even integral "n" possesses only odd harmonic distortion at its output. Fig. 5 shows that the third harmonic distortion in square law operation is higher than that in linear operation. Peaks in the frequency response occur for $\Delta w/w_0 = \pm 2g_1/(2n+1)$. The discriminator sensitivity in linear operation is given by

$$S_{\text{lin}} = (-1)^{n/2} \eta_2 V_0 (2n+1)\pi/(2\sqrt{2}\, w_0 g_1).$$

IV. Experiment

A schematic diagram of the experimental setup is shown in Fig. 1. The tunable high-Q Gunn oscillator (0902 EC X-480B) using Microwave Associates' Gunn diode (No. MA 49104) served as the source of coherent carrier. The Marconi AM–FM signal source (Model 6158A) having a frequency modulation sensitivity of 2 MHz/V and a maximum frequency modulation rate of 0.1 MHz is used as the FM generator. Any reflection from the detector connected with the E-arm of the magic tee is eliminated by the isolator preceding it. The lockband of the oscillator is reduced sufficiently by attenuating the strength of the synchronizing signal. The Q-factor and the free-running output power of the Gunn oscillator are 2198 and 58 mW, respectively. Total lockband of the Gunn oscillator is 0.25 MHz for a CW injection power of 0.2 mW at 9.356 GHz.

V. Discussion and Conclusion

Symmetrical tuning of the adjustable diode detectors is very important for producing maximum linearity in the response of the discriminator. A high-Q passive resonant cavity tuned at the FM carrier frequency can be placed before the narrow-band Gunn oscillator in order to achieve a better sideband suppression. Low index, fast modulation is preferred for this technique since low index of modulation produces less harmonic distortion at the discriminator output, while fast modulation produces strong sideband suppression.

References

[1] R. V Pound, "Electronic frequency stabilization of microwave oscillators," *Review of Scientific Instruments*, vol. 17, pp 490–505, Nov 1946.

[2] C. K Chan and R S. Cole, "A stable microwave integrated circuit X-band Gunn oscillator," *IEEE Trans. Microwave Theory Tech.*, p. 815, Aug. 1974.

[3] C. W. Lee and W. Y. Seo, "Super wide-band FM line discriminator," *Proc. IEEE*, pp. 1675–1676, Nov. 1963

[4] C. W Lee, "An analysis of a super wide-band FM line discriminator," *Proc. IEEE*, pp. 1034–1038, Sept 1964.

[5] R J. Mohr, "Broad-band microwave discriminator," *IEEE Trans Microwave Theory Tech.*, pp. 263–264, July 1963

[6] S J. Robinson, "Comment on broad-band microwave discriminator," *IEEE Trans on Microwave Theory Tech.*, pp 255–256, Mar 1964.

[7] E. H. Katz and H. H. Schreiber, "Design of phase discriminators," *Microwaves*, pp 26–33, Aug 1965.

[8] L. I Reber, "Improved performance in phase discriminators," *Microwaves*, pp. 48–52, May 1971

[9] M L Sisoida and O. P. Gandhi, "Octave bandwidth *L*- and *S*-band stripline discriminators," *IEEE Trans Microwave Theory Tech.*, pp 271–272, Apr. 1967

[10] S. R Mishra and R P Wadhwa, "Development of an *X*-band waveguide frequency discriminator," *IEEE Trans. Microwave Theory Tech.*, pp. 660–661, Sept 1970.

[11] W Y Seo, "Microwave discriminator for above 10 Gc," *Proc. IEEE*, p. 179, Feb. 1965.

[12] R. L Addington, "Comments on 'microwave discriminator for above 10 Gc' & 'stripline phase shifter,'" *Proc. IEEE*, p 1229, Sept. 1965

[13] J Nigrin, N. A Mansour, and W. A. G Voss, "Single hybrid tee frequency discriminator," *IEEE Trans. Microwave Theory Tech.*, pp 776–778, Sept. 1975

[14] P. Z. Peebles, Jr and A H. Green, "A microwave discriminator with easily adjusted bandwidth," in *Proc. of Southeast Conf.*, Roanoke, VA, 1979, pp. 275–277

[15] P Z. Peebles, Jr. and A. H Green, Jr., "A microwave discriminator at 35 GHz," *Proc IEEE*, pp. 286–288, Feb 1980.

[16] B. Glance, "Digital phase demodulator," *Bell Syst. Tech. J*, pp. 933–949, Mar 1971

New Concepts in Traveling-Wave Amplifiers

M. FRIEDGUT

Abstract—**Two new networks with the potential for good port VSWR over very broad bandwidths are proposed for use in both low-power balanced amplifiers, and high-power combining systems. These new structures which are called Low-Sidelobe and Squintless Traveling-Wave Amplifiers (LSTWA and SQTWA, respectively) have been derived from conventional Traveling-Wave Amplifiers (TWA) by utilizing Phased Array Antenna concepts and design techniques. Using Monte-Carlo simulations the relative performance of the three structures is compared. Finite loss and mismatch effects are also considered.**

I. Introduction

Wide bandwidth requirements in low-noise/low-power amplifiers have generally been met by using multisection Lange couplers to realize cascadable low VSWR-balanced modules. Active devices covering the full 2–20 GHz frequency range are routinely available today [1] and thus the coupler performance is often the limiting factor in such designs [2].

High-power requirements over wide bands on the other hand, generally lead to the use of combiner networks to achieve the desired power levels [3], [4]. In monolithic designs, the traveling-wave structure [5] is a promising contender.

In the following sections, the conventional TWA is compared with the LSTWA and SQTWA structures. Design and analysis methods from Phased Array theory provide insight into the combining and matching properties of all these devices.

In Section II, expressions will be developed for the input reflection-coefficient and forward transmission coefficient for the

Manuscript received January 18, 1985; revised November 18, 1985

The author is with AWA Communications Laboratory, North Ryde, 2113, N.S W Australia

IEEE Log Number 8407187